2013

AVHRR-NDVI-based crop coefficients for analyzing long-term trends in evapotranspiration in relation to changing climate in the U.S. High Plains

Denis Mutiibwa
University of Nebraska-Lincoln

Suat Irmak
University of Nebraska-Lincoln, suat.irmak@unl.edu

WATER RESOURCES RESEARCH, VOL. 49, 231–244, doi:10.1029/2012WR012591, 2013

AVHRR-NDVI-based crop coefficients for analyzing long-term trends in evapotranspiration in relation to changing climate in the U.S. High Plains

Denis Mutiibwa[1] and Suat Irmak[1]

Received 26 June 2012; revised 7 November 2012; accepted 14 November 2012; published 24 January 2013.

[1] Studies in regions of extensive irrigation practices have revealed a significant influence of evaporative cooling on regional temperatures as a result of surface energy redistribution during evaporation. In the U.S. High Plains, maximum temperatures during the last quarter of the 20th century have been decreasing. We investigated the trends in evapotranspiration (ET or latent heat) fluxes originating from increasing irrigation practices in the High Plains region from 1981 to 2008. We estimated actual ET (ET*c*) over the entire High Plains from the spatial crop coefficients (K*c*) and spatial reference (potential) ET (ET*ref*). We proposed and validated a global linear relation between K*c* and advanced very high resolution radiometer-based normalized difference vegetation index. Our results show an increase in ET*c* trends over the region in the last three decades. The study shows that the increase in ET*c* flux was not in principal from increased atmospheric evaporative demand. Rather, the increase in ETc was due to significant increase in irrigated surfaces. The increase in ETc fluxes is likely a manifestation of increased redistribution of surface energy into latent heat and less partitioning into the sensible heat. We investigated the evolution of full canopy cover vegetation (normalized difference vegetation index >0.70) in relation to the maximum temperature anomalies during the study period. Results revealed a significant negative correlation between the two variables. These results appear to demonstrate that there is a regional evaporative cooling signal due to extensive irrigation practices, which impacts regional temperatures during the summer seasons.

Citation: Mutiibwa, D., and S. Irmak (2013), AVHRR-NDVI-based crop coefficients for analyzing long-term trends in evapotranspiration in relation to changing climate in the U.S. High Plains, *Water Resour. Res.*, *49*, doi:10.1029/2012WR012591.

1. Introduction

[2] Climate change has been projected to impact regional temperatures, rainfall distribution, and atmospheric water vapor content and resulting hydrologic parameters such as infiltration, surface runoff, stream flow, deep percolation, etc. Atmospheric water vapor, a major component of the hydrological cycle, has been anthropogenically altered, in part, by land use/land cover changes such as conversion of natural vegetation to farmlands, urbanization, irrigation practices, afforestation, and deforestation. These land use/land cover changes influence atmospheric water vapor content through modification of surface properties and evaporation [*Pielke et al.*, 2002]. In agriculture-dominated regions, massive increase in regional water vapor is considered to be evapotranspiration (ET) from irrigated vegetation surfaces as a result of increased soil surface evaporation and transpirative losses from the vegetation. Studies have found that, in regions where extensive irrigation is practiced, surface temperatures have been significantly impacted due to energy balance redistribution during evaporation [*Boucher et al.*, 2004; *Kueppers et al.*, 2007; *Lobell et al.*, 2009]. *Pan et al.* [2004] observed a minimal warming region (warming hole) in the central United States due to evaporative cooling suppressing daytime maximum temperatures over the region during the summer months. The study revealed a suppressed increase in daily maximum surface temperatures over the warming hole of less than 0.5 K, substantially less than the mean increase of about 3 K over the continental United States. D. Mutiibwa (Identifying changes in climatic trends and the fingerprints of landuse and landcover changes in the high plains of the USA, unpublished Ph.D. dissertation, 2011) investigated the trends in the High Plains regional temperatures, and the results showed a nonsignificant decreasing trend of 0.004°C yr^{-1} in maximum temperature over the High Plains region during the last quarter of the 20th century. In a more localized study of the agroecosystem-dominated Platte River Basin of central Nebraska, *Irmak et al.* [2012] observed that the maximum air temperature had a nonsignificant decreasing trend of 0.0089°C yr^{-1} for the 116 year period from 1893 to 2008. However, they observed

[1]Department of Biological Systems Engineering, University of Nebraska-Lincoln, Lincoln, Nebraska, USA.

Corresponding author: S. Irmak, Department of Biological Systems Engineering, University of Nebraska-Lincoln, 239 L.W. Chase Hall, Lincoln, NE 68583, USA. (sirmak2@unl.edu)

0043-1397/13/2012WR012591

a significant increase in minimum and mean temperatures at a rate 0.038°C yr^{-1} and 0.0187°C yr^{-1}, respectively. *Folland et al*. [2001] also observed the cooling of the central United States by 0.2–0.8 K in the summer months. The decreasing trend in maximum temperature was attributed to the atmosphere-hydrology feedback effect of evaporative cooling from increase in irrigated land area in the region during the summer irrigation season. In this study, we investigate the trends in ET or latent heat due to increasing irrigation practices in the High Plains region over the period of 1981 to 2008. Although the response of climate to irrigation can be expected to vary by region [*Lobell et al*., 2009], increasing actual evapotranspiration (ET*c*) indicates a mechanistic surface energy redistribution into latent heat flux, which has resulted into suppressed warming over the High Plains. However, studies that quantified the impact(s) of irrigation development on regional and local temperature and ET*c* respond in heavily irrigated regions are extremely limited.

[3] This study estimated ET*c* using the two-step approach, in which reference (potential) evapotranspiration (ET*ref*) is computed and adjusted with the crop-specific ET*c* estimates using crop coefficients (K*c*). ET*ref* is a climatic variable that defines the evaporative demand of the atmosphere over a reference vegetation surface [*Irmak et al.,* 2012]. *Hargreaves and Samani* [1985] empirical method was used to estimate ET*ref* for a grass-reference surface (ET*o*) using the minimal available climatic variables recorded for a long period (30 years) at all weather stations in the study area. Several authors have recommended the *Hargreaves and Samani* [1985] method in situations where climate data are limited [*Xu and Singh*, 2001] to estimate reference (potential) ET.

[4] *Doorenbos and Pruitt* [1979] and *Wright* [1982] published K*c* values for a variety of vegetation surfaces. The advent of remote sensing application in water resources assessments, planning, and management initiated a potentially effective methodology of estimating K*c* values for various vegetation surfaces over small or large areas. Using Landsat satellite imagery, *Singh and Irmak* [2009] successfully developed a regression vegetative index model to estimate K*c* for several major crops (maize, soybean, sorghum, and alfalfa) grown in Nebraska. Our study developed a regression model to estimate spatial K*c* from (normalized difference vegetation index (NDVI)) obtained from National Oceanic and Atmospheric Administration (NOAA) satellite-acquired advanced very high resolution radiometer (AVHRR). The model was applied to estimate spatial K*c* for the High Plains region, for the growing seasons of 1981 to 2008. The summer months studied (June–August) are considered to be the peak irrigation months of the growing season, which is typical in Midwestern and High Plains region in the United States. The estimated spatial K*c* values were used to adjust the spatial ET*o* estimates, producing spatial growing season ET*c* maps for the High Plains. Specific objectives of this study were as follows: (i) develop spatial ET*o* from *Hargreaves and Samani* [1985] method, (ii) estimate spatial K*c* from satellite-acquired NDVI data, (iii) estimate spatial growing season ET*c*, and (iv) evaluate the trends in growing season ET*c* in relation to regional temperature changes over the period of 1981–2008 in the High Plains region of the United States.

2. Materials and Methods

2.1. Study Area

[5] The study area is the High Plains of the United States (Figure 1). *Rossum and Lavin* [2000] described the region as geographically located in central United States between dense eastern forests and the western mountains and deserts. The area is a vast, flat-to-rolling plain that is predominately agricultural, including rangeland, natural prairie, irrigated, and rainfed farming of agronomic row crops mainly maize, soybean, sorghum, alfalfa, winter wheat, sugar beets, and cotton. Precipitation is limited in the western plains and increases toward the east. The average annual precipitation received ranges from approximately 260 mm in the west to 600 mm in the east. Temperature has a strong north-south gradient. The climate is influenced by the cold air fronts from Canada in the north and Rocky Mountains in the northwest, as well as humid and warm air masses flowing into the region from the Gulf of Mexico from the south [*Irmak,* 2010; *Irmak et al*., 2012]. The region is periodically affected by droughts, which likely stirred the region into extensive irrigation during the 1950s–1960s [*Rhodes and Wheeler*, 1996].

2.2. Input Data

2.2.1. Temperature Data

[6] The U.S. Historical Climatology Network (USHCN) was the source of the monthly mean, minimum, and maximum temperature data set for 204 weather stations used in the study. The USHCN data sets were obtained from the National Climatic Data Center (NCDC) [*Smith et al*., 2008; http://www.ncdc.noaa.gov]. Figure 1 shows the locations of the weather stations that were used in the analyses on the regional map of High Plains. For data quality, USHCN subjects the climatic data sets to a comprehensive quality control, inspection, inhomogeneity correction, and removal of all monthly mean outliers that differed from their climatology by more than 2.5 standard deviations [*Peterson and Vose*, 1997]. In the case of missing data, the USHCN uses the network of surrounding weather stations to interpolate the missing values, thus producing a complete temperature data set.

2.2.2. ET Measurements

[7] Measured surface energy fluxes, including ET*c* (latent heat), sensible heat flux, soil heat flux, net radiation, and other climatic variables, were obtained from the Nebraska Water and Energy Flux Measurement, Modeling, and Research Network (NEBFLUX) [*Irmak*, 2010]. NEBFLUX is a comprehensive network of 10 Bowen ratio energy balance system (BREB) and three eddy covariance system (ECS) towers installed on vegetation surfaces ranging from tilled and untilled irrigated and rainfed croplands, including irrigated alfalfa, rainfed switchgrass, rainfed winter wheat, irrigated, and rainfed grasslands, irrigated seed maize-cover crop rotation to Phragmites-dominated Cottonwood and Peach-leaf willow riparian plant communities. In NEBFLUX, all energy balance and microclimatic and soil water content variables are measured continuously throughout the year on an hourly basis. Measurements and observations of the soil characteristic, year-long hourly soil moisture content every 0.30 m up to 1.8 m in soil profile, vegetation physiology, leaf area index, plant height, yield, and biomass

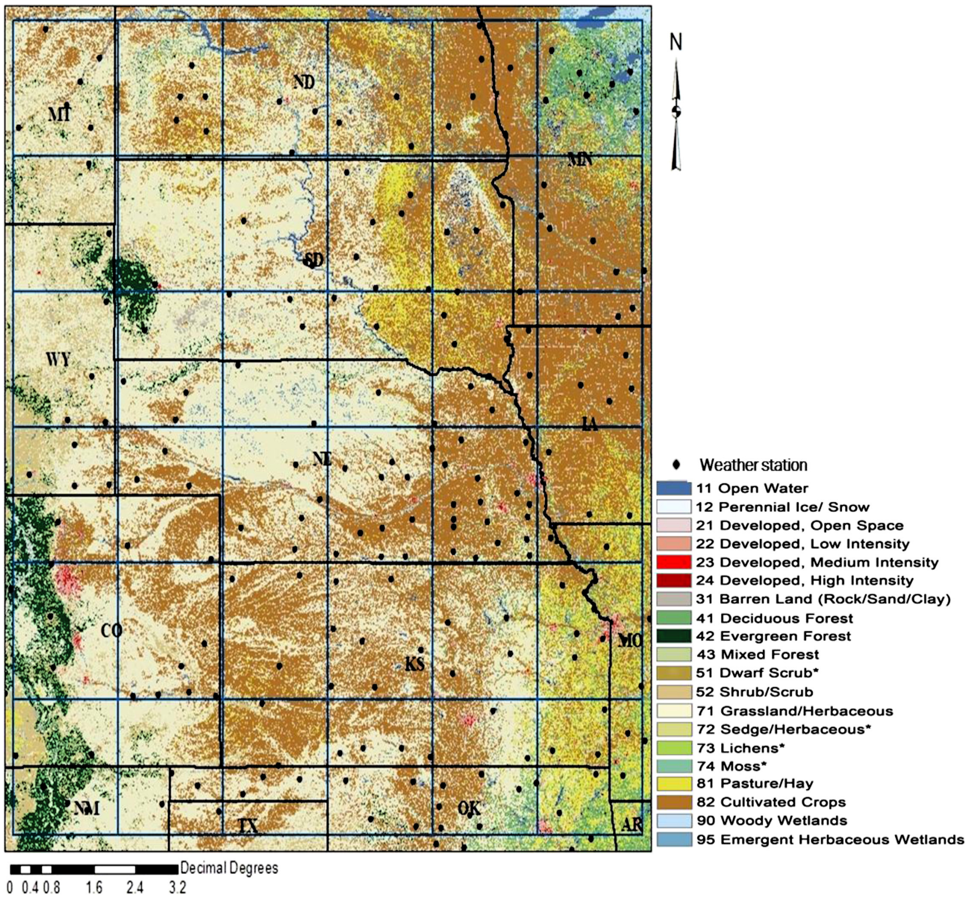

Figure 1. High Plains land cover during 2006 (source: National Land Cover Database, http://www.mrlc.gov/nlcd06_data.php) and the weather stations (black dots) used in the analysis.

production are also conducted in the NEBFLUX sites through extensive field campaigns. Detailed information of BREBS and ECS measurements, including instrumentation details, site characteristics, etc., are provided by *Irmak* [2010]. For this study, we used the data sets from five of NEBFLUX towers to develop the K*c*-NDVI relationship. The information about the installation dates, latitude, longitude, elevation, and vegetation surface cover of the five BREBSs that are used in this study is presented in Table 1. The locations of the five BREBSs that are used in this study are shown in Figure 3a.

2.2.3. NDVI Data

[8] The NDVI data were obtained from the Global Inventory Modeling and Mapping Studies (GIMMS). The AVHRR-based data were acquired by NOAA polar-orbiting satellites that have a biweekly temporal resolution and 4 km onboard resampled spatial resolution. GIMMS data are resampled to 8 km pixel size products. The special features of the GIMMS data include reduced NDVI variation arising from calibration, view geometry, volcanic aerosols, and other effects that are not related to actual vegetation change. The cloud-free composite images were constructed at regular interval by selecting pixels with the maximum NDVI during regularly spaced intervals. More detailed information on radiometric calibration, atmospheric correction and cloud screening, satellite drift correction, intercalibration of NDVI, and quality assessment of the data is described by *Pinzon et al*. [2004] and *Tucker et al*. [2005].

2.3. Hargreaves and Samani Reference (Potential) ET Equation

[9] Estimating ET*c* for a specific crop using the two-step procedure [*Irmak et al.,* 2012] requires computing ET*ref* for a reference crop (grass or alfalfa). Several methods

Table 1. Vegetation Surface and Coordinates of the BREBS From the NEBFLUX Project Used as a Ground-Truth, Modeling, and Validation of the K*c*-NDVI Relationship

BREBS	Vegetation Surface	Installation Date	Latitude	Longitude	Elevation (m)	Use
BREBS-1	Irrigated soybean/maize rotation	13 October 2004	40.58	98.13	552.0	Calibration
BREBS-2	Irrigated and grazed grassland	25 September 2007	41.28	97.94	577.3	Validation
BREBS-3	Rainfed/grazed grassland	13 March 2008	41.27	97.95	549.0	Calibration
BREBS-4	Irrigated soybean/maize rotation	10 June 2008	40.58	97.65	573.6	Calibration
BREBS-5	Irrigated soybean/maize rotation	9 July 2008	40.57	97.65	576.0	Calibration

have been developed to estimate ET*ref* with different number of input climatic variables and levels of accuracy. *Hargreaves and Samani* [1982, 1985] at Davis, CA, developed a grass-reference ET*o* equation that only requires air temperature and extraterrestrial radiation (RA) as input climate variables. The other variable of the equation is the difference between mean monthly maximum and mean monthly minimum temperature (TD) and the form of the equation used in this study is as follows:

$$\mathrm{ET}o = 0.00023 \times \mathrm{RA} \times \mathrm{TD}^{0.5}(T + 17.8), \quad (1)$$

where ET*o* is the monthly average grass-reference ET (mm d^{-1}), T is the monthly average air temperature (°C), and RA is in mm d^{-1}. RA is computed from latitude of the sites and day of the year as presented in *Hargreaves and Samani* [1985].

[10] ET*o* was estimated for June–August from 1981 to 2008 at 204 weather stations. For each month, a spatial ET*o* surface was generated over the High Plains region using ArcGIS spline geostatistical interpolation tool. The grid size of the ET*o* interpolated raster maps was 8 km to match the grid size of the NDVI rasters. The spatial ET*c* was then estimated as a product of spatial ET*o* and spatial K*c*.

2.4. Crop Coefficient and NDVI Relationship

[11] We estimated spatial K*c* by developing a relationship between K*c* and NDVI. The development of the K*c*-NDVI model required ground-truth data of measured K*c* values at different locations. The measured K*c* values over various vegetation surfaces during the growing period of 2008 were obtained from the five NEBFLUX BREBSs located in south-central Nebraska [*Irmak*, 2010]. The measure K*c* was obtained as quotient of measured ET*c* and estimated ET*o*. The K*c*-NDVI model was calibrated at four NEBFLUX sites as indicated in Table 1. The vegetation surfaces sampled for K*c*-NDVI relationships included irrigated maize, irrigated soybean, irrigated mixed grassland (tall fescue, *Festuca arundinacea*; Kentucky bluegrass, *Poa pratensis*; smooth bromegrass, *Bromus inermis*; and creeping foxtail, *Alopecurus arundinacea*), and rainfed grassland of native Buffalograss (*Bouteloua dactyloides Nutt*) [*Irmak,* 2010]. Daily-measured K*c* values at each BREBS site for June–August were aggregated into biweekly K*c* values to fit the NDVI data temporal resolution. The first 15 days of the month were averaged for the first biweekly K*c* value, and the following 15 or 16 days were averaged for the second biweekly K*c* value. In total, 22 aggregated K*c* values at the four NEBFLUX BREBS sites were used to calibrate the K*c*-NDVI model in the growing season of 2008.

[12] Using ArcGIS pixel sampling tool, the NDVI values of the pixels with the BREBS sites were sampled. The NDVI data are on a biweekly basis; therefore, two values from each of the 3 study months were sampled. Given that the NDVI data have spatial resolution of 8 km, the NDVI value of each pixel represents the average vegetation coverage of the entire pixel. Therefore, the assumption here is that the aggregated K*c* values were representative of the vegetation surfaces in the fields within 8 km as captured by the NDVI pixel. Using the measured K*c* values and corresponding NDVI data from the observation fields, a linear regression equation was developed as

$$Kc = 1.58\mathrm{NDVI} - 0.111. \quad (2)$$

The model has a coefficient of determination (r^2) of 0.71, modeling efficiency (EF, defined later in equation (3)) of 0.70, and root-mean-square difference (RMSD) of 0.14 between BREBS-measured and BREBS-estimated K*c* (Figure 2a).

[13] Equation (2) was calibrated using data from BREBS-1 (2008), BREBS-3 (2008), BREB-4 (2008), and BREBS-5 (2008) and validated using the data from BREBS-1 (2006 and 2007) and BREBS-2 (2008) to evaluate its performance at estimating K*c*. Similar steps as discussed above to obtain biweekly aggregated K*c* values and sampling of corresponding NDVI pixels values were followed up for the 3-year used in the validation of equation (2). Figure 2b shows the linear fit of estimated and aggregated K*c* values. The equation had r^2 of 0.72, EF of 0.65, and RMSD of 0.12, which indicate a good validation performance for the model. The strong relationship between NDVI and K*c* enabled other studies to develop linear models predicting K*c* for various vegetation canopies. Several studies [*Neale et al.*, 1989; *Hunsaker et al.*, 2005; *Singh and Irmak*, 2009]

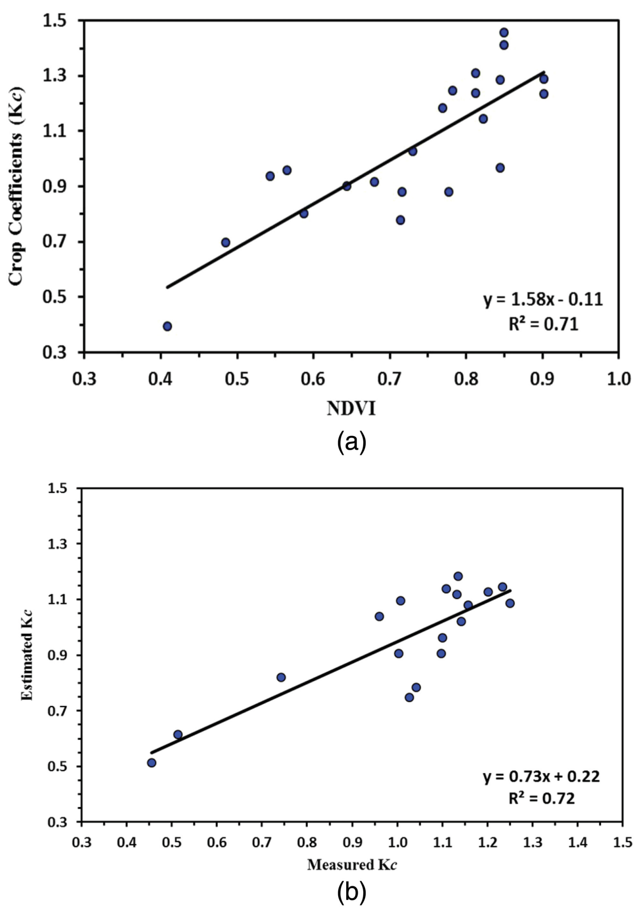

Figure 2. (a) Linear relationship between NDVI and NEBFLUX-BREBS-measured K*c* used in the calibration of equation (2). (b) Regression between NDVI-based K*c* and NEBFLUX-BREBS-measured K*c* for the validation of equation (2).

have achieved good results in predicting spatial K*c* from NDVI using linear models. The models have shown to perform better when they are crop specific. For instance, *Singh and Irmak* [2009] produced results of r^2 between 0.83 and 0.90 for models developed specifically for soybean, maize, and sorghum. Despite enhanced performance, developing several models for different vegetation types and field management practices may be impractical when working over large regions such as the High Plains. For that reason, developing a well-calibrated single model may be the compromise between applicability and precision in cases of large spatial domains.

2.5. Statistical Analyses

[14] *Willmott* [1982] demonstrated that using only correlation measures, such as r^2, is insufficient in proving the adequacy and efficiency of model performance. Thus, the performance of the developed K*c*-NDVI model to estimate spatial K*c* was further quantitatively analyzed using two statistics: the (RMSD, used as a measure of the total difference between the estimated and measured K*c* values; and the EF used to assess the fraction of the variance of the measured values explained by the model. The EF ranges from 1 to negative infinite, with values closer to 1, indicating good performance of the model. The EF is the ratio of the mean square error to the variance in the observed data, subtracted from unity, as

$$\mathrm{EF} = 1 - \frac{\sum (O_i - P_i)^2}{\sum (O_i - \overline{O})^2}, \tag{3}$$

where O_i and P_i are the measured and estimated K*c* values, respectively, and $\overline{O}$ is the mean of measured data. All trends in ET*c* and temperature were tested for significance at the $\alpha = 0.05$ level.

2.6. Spatial Growing Season ET

[15] Spatial ET*c* was estimated as a product of spatial ET*o* and spatial K*c*. In this study, the growing season ET*c* represents the sum of the ET*c* estimate for the typical intensive irrigation months of June–August in the High Plains. Both ET*o* and K*c* have a spatial grid size of 8 km, and, therefore, the estimated ET*c* has a spatial grid size of 8 km. From the two K*c* values estimated per month, the total monthly ET*c* was estimated as

$$\text{Monthly ET}c = n_1 \times \mathrm{K}c_1 \times \mathrm{ET}o + n_2 \times \mathrm{K}c_2 \times \mathrm{ET}o, \tag{4}$$

and growing season ET*c* was determined as

$$\text{Growing season ET}c = \mathrm{ET}c_{\mathrm{June}} + \mathrm{ET}c_{\mathrm{July}} + \mathrm{ET}c_{\mathrm{August}}, \tag{5}$$

where n_1 is 15 (days), and n_2 is 15 or 16, depending on the number of days in the month. Kc_1 and Kc_2 represent the first and second estimated K*c* values of the month. The growing season ET*c* was estimated as the sum of June–August monthly ET*c* for the period of 1982 to 2008. NOAA's AVHRR satellites started acquiring NDVI data in July 1981; therefore, growing season ET*c* for the year 1981 was summed from ET*c* estimates of only July and August.

3. Results and Discussion

3.1. Reference ET

[16] The maps of spatial ET*o* for 1982, 1990, 2002, and 2008 are presented in Figures 3a–3l. ET*o* over the High Plains ranged between 3 and 9 mm d^{-1}. For June, ET*o* was generally lower than the values in July and August due to lower levels of incoming shortwave radiation. During June, ET*o* appeared to increase from north to south. This is, in part, due to the incoming cool air masses from Canada, which prevail over the Dakotas, resulting in cool temperatures in the High Plains, thus lowering the atmospheric evaporative demand in the northern part of the High Plains region. For July and August, there is no characteristic spatial trend in ET*o* over the High Plains. However, the central and eastern Colorado regions show a consistent pattern of lower ET*o* values. *Mutiibwa* [2011] observed that eastern Colorado was also considerably cooler relative to other parts of the region. This was, in part, attributed to, first, the high elevation effect on temperatures in the region, the elevation of weather stations in the region were between 1600 m and 2600 m. Second, because of the region's location being on the foothills of the Rocky Mountains, it is subjected to periodic and severe turbulent mixings conditions from the effects of strong westerly winds over the mountain barrier. The winds are associated with a strong cold frontal passage downslope off of the mountains; thus, the summer temperatures are generally cooler on the eastern slopes. Given that our ET*o* estimation procedure is temperature based, lower temperatures results in lower ET*o* estimates.

3.2. Trends in Grass-Reference ET (ET*o*)

[17] The trends in ET*o* over the study period (1981–2009) were assessed by selecting six pixels from different locations of the High Plains. The six pixels were selected based on land use maps of 1982, 1990, 2002, and 2008. For accurate trends in ET*o*, it is important that the surface characteristics over the six sampled locations are almost consistent over the 28 years. The pixels were at least 90% agricultural fields during the 4 years mentioned above. The assumption is that, over the entire study period, the land use coverage was at least 90% cropland. The land use maps were part of the University of Nebraska-Lincoln, Center for Advance Land Management Information Technologies (CALMIT)-developed land cover databases. The threshold of 90% ensured that the pixels had minimal nonvegetation surface changes; thus, the areas in the pixels were mostly cultivated and vegetated during the study period. The location of the six pixels is shown in Figure 3a. The trends of monthly average daily ET*o* (mm d^{-1}) for June–August are presented in Figures 4a–4c. Except during the summer season of 1988, which was an extreme drought season, ET*o* for June was less than July and August at all six locations. During the summer season of 1988, the monthly average temperatures of June were unusually greater than July and August average temperatures. At all six locations shown on Figures 4a–4c, ET*o* for June ranged between 4.3 mm d^{-1} at location (C) in 1998 and 7.7 mm d^{-1} at location (F) in 1988. However, taking out the drought year of 1988, the greatest ET*o* estimate in June was 6.6 mm d^{-1} in 2006 at location (D). ET*o* in July ranged between 5.5 mm d^{-1} in

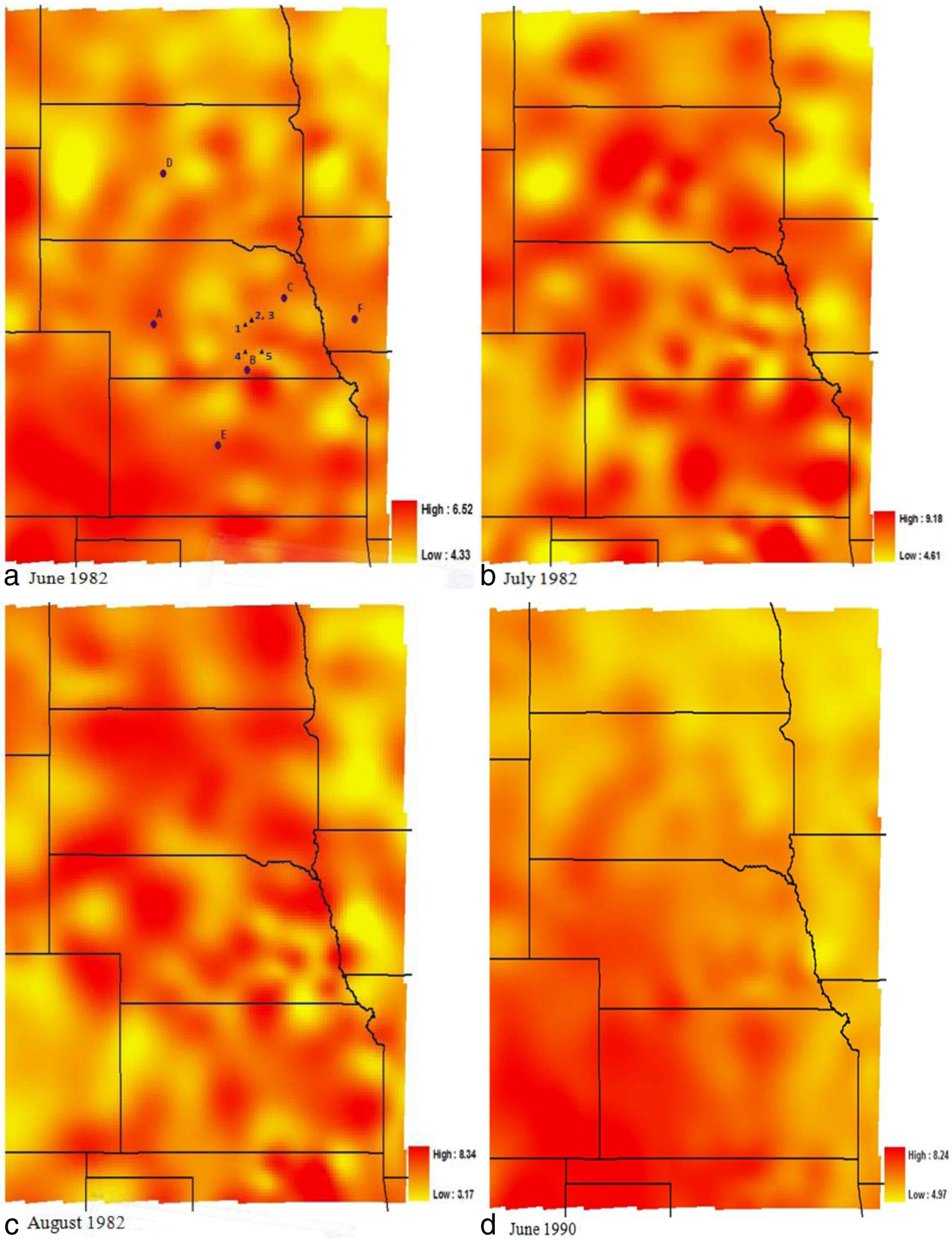

Figure 3. (a–l) Monthly spatial distribution of ET*o* (mm day^{-1}) in June–August for 1982, 1990, 2002, and 2008. Figure 3a shows the location of the five BREBS towers and the six sampled locations. (Continued on next page.)

1982 at location (F) and 8.2 mm d^{-1} in 1998 at location (B). For August, the ET*o* range was 4.1 mm d^{-1} in 1985 at location (A) and 7.5 mm d^{-1} in 1983 at location (A). Location (D) in August has lower ET*o* trend relative to other locations, which could be related to cooler temperatures in South Dakota, because it is the furthest point to the north. *Waltman et al*. [2003] studied the recent droughts in the Nebraska using soil moisture regimes as drought risk indicator and showed that the recent droughts occurred in 1988, 1989, 1991, 1995, 1999, and 2000. Although their study focused on Nebraska, it is most likely that the droughts and the impacts were on a regional scale. In fact, the drought of 1988 covered 36% of the United States at its peak [*Riebsame et al*., 1991]. In our study, June depicts some of the droughts over the region mentioned in the *Waltman et al*. [2003] study, including the recent severe drought of 2002. The droughts of 1999–2000 were, on the other hand, depicted by August. The trends in ET*o* are shown in Figures 4a–4c as regression dashed lines. The slopes of the regression line represent the simple quantitative measure of the trends. The slopes were all close to zero (or no trend) and insignificant ($p > 0.05$). Therefore, there is no increasing or decreasing trend in ET*o* over the study years. This could be due to the noise in the ET*o* estimates that overwhelms the trend or the number of years may be insufficient for a significant trend. Figure 4 also reveals a considerable amount of fluctuations in ET*o* over the 28 year period due to the droughts and cool summers.

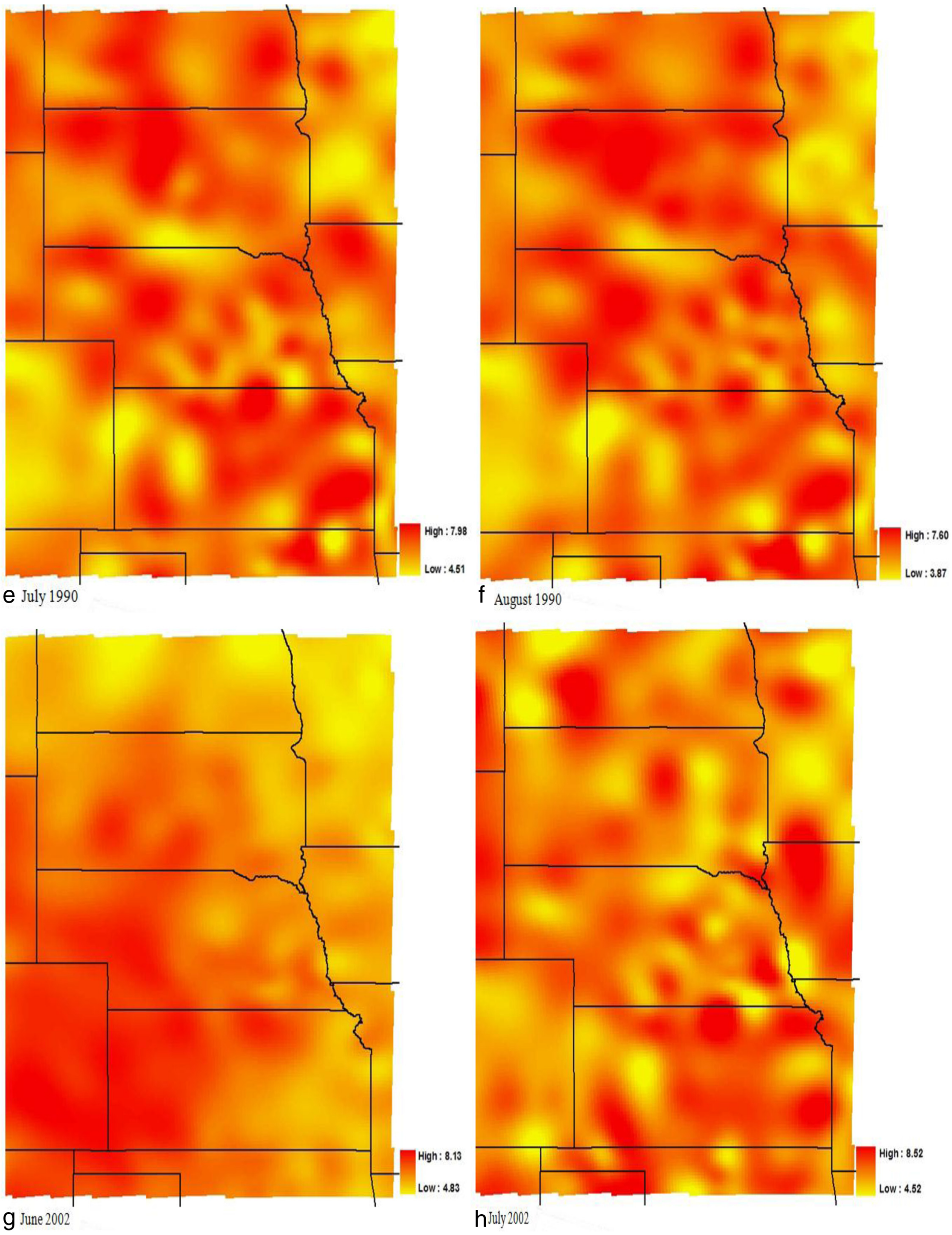

Figure 3. (continued)

3.3. Crop Coefficients

[18] Figures 5a–5d show the validation of the K*c* model for the summer seasons of 2006, 2007, and 2008 at the BREBS-1 and BREBS-2 locations. Figure 5a shows the model's estimates of K*c* from June to August in 2006 at BREBS-1 site. In 2007, at BREBS-1 site (Figure 5b), the model also produced a good performance in estimating K*c*, although it slightly overestimated through mid-July and underestimated through August. In 2008, at BREBS-2 site (Figure 5c), the model underestimated K*c* almost during the entire 3 months of the growing season. Figure 5d shows the linear regression of estimated K*c* and measured K*c* for the three validation scenarios. The results of r^2 for the validations were good; 0.92 at BREBS-1 (2006), 0.94 at BREBS-1 (2007), and 0.91 at BREBS-2 (2008). Thus, the K*c*-NDVI model was able to explain more than 90% of the variability in measured K*c* at two independent sites during three independent growing seasons. At BREBS-2 (2008), the model overestimated K*c* due to minimal variability and development in perennial irrigated grass K*c* at the site, whereas the NDVI value from the pixel changes due to probable crop development and its variability in the surrounding fields.

3.4. Spatial Growing Season Actual ET

[19] The ultimate goal of this study was to estimate spatial growing season ET*c* in the High Plains region and relate its trends to temperature trends during the period of 1981 to 2008. In this section, four spatial ET*c* maps are presented in Figure 6 for the same years as ET*o* maps

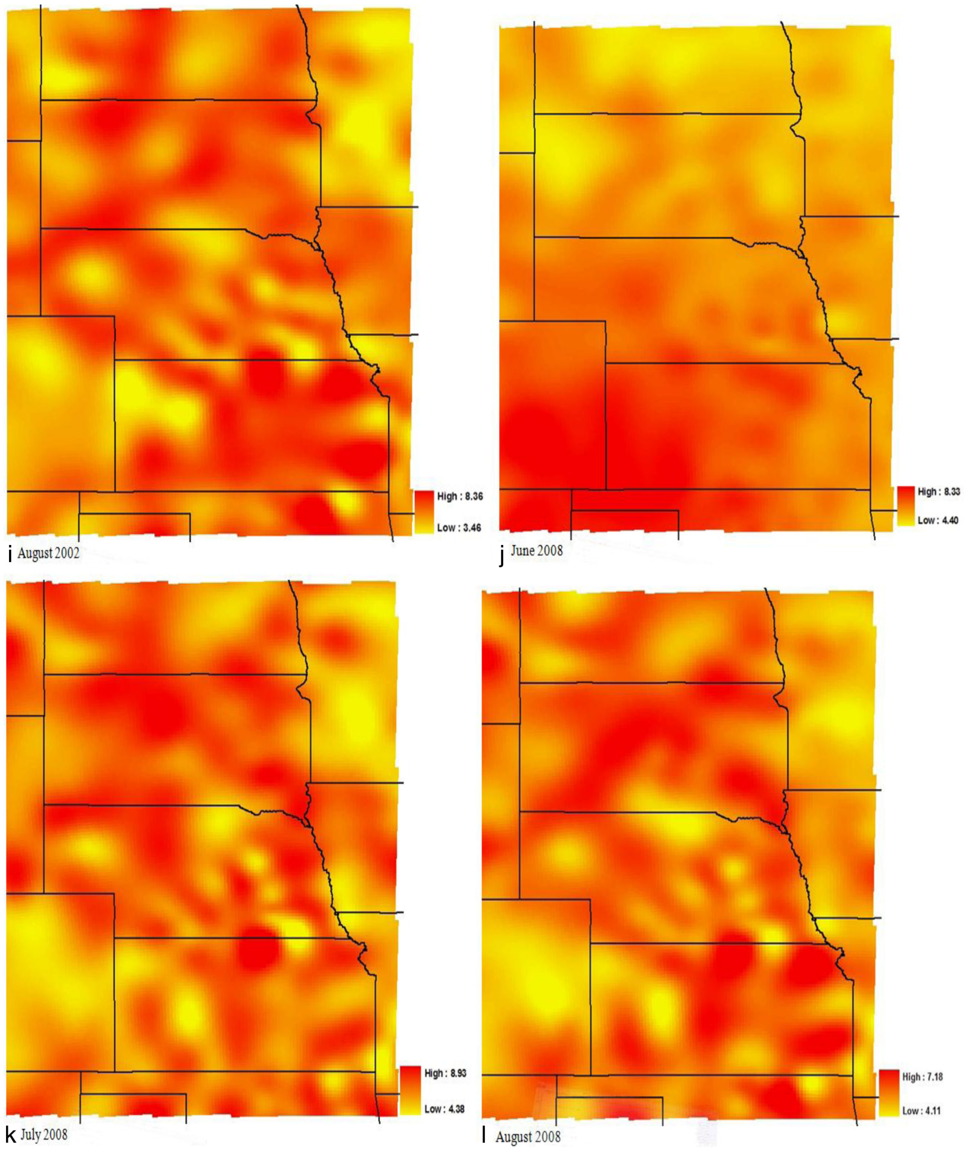

Figure 3. (continued)

presented in Figure 3. The four figures developed (Figure 6) show that growing season ET*c* increases significantly from the central to eastern part of the region. The High Plains region rainfall distribution decreases from east to west. Therefore, there is more rainfed agriculture in the east than in the central and western parts of the High Plains where most of the irrigation is practiced. Due to the precipitation distribution, the natural vegetation is more vigorous in the east than in the west, and our study area is in the transition between the dense eastern forests and the western mountains and deserts. Because precipitation and NDVI mainly increases from west to east and K*c* is positively related to NDVI (equation (2)), the spatial distribution of K*c* also increases from west to east. Thus, the growing season ET*c* mostly has similar spatial distribution as precipitation and NDVI. The growing season ET*c* ranged from 0 to about 780 mm season^{-1}. Negative spatial ET*c* values observed in 2002 and 2008 (i.e., Figures 6b and 7c) originate from the negative NDVI values. The NDVI values for snow cover are negative, and in the Figures 6b and 7c, the negative values observed in the Rocky Mountains where there are snow caps even during some of the summer months. In addition, the negative ET*c* values could originate from bare soil NDVI values. The NDVI values for bare soil are positive but usually very low or close to zero. Since our K*c*-NDVI relationship has a negative intercept, K*c* values for bare soil could also yield negative ET*c* values. For the most part, eastern Colorado had the lowest growing season ET*c* estimates for all the study years. In Figure 3, the ET*o* maps for July and August also showed that eastern Colorado had the lowest ET*o*.

3.5. ET*c* and Temperature Trends

[20] The trends in growing season ET*c* in the region were examined using the six sampled locations that were already studied for ET*o* and K*c* evolution. The trends of

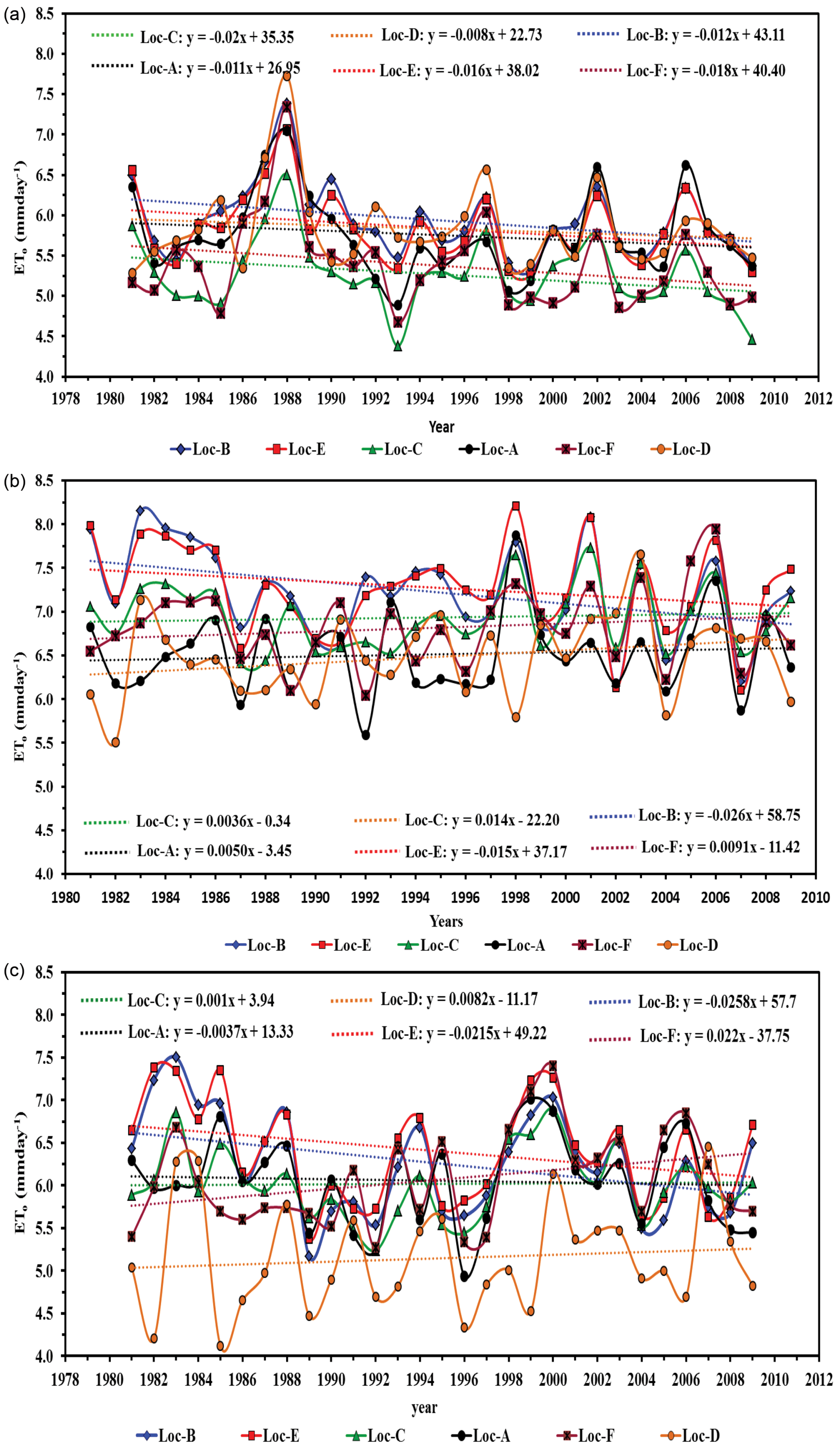

Figure 4. Time series of monthly average daily ET*o* from 1981 to 2009 at the six sampled locations in the U.S. High Plains: (a) June, (b) July, and (c) August. The dashed regression lines represent the trend in ET*o* during the same period.

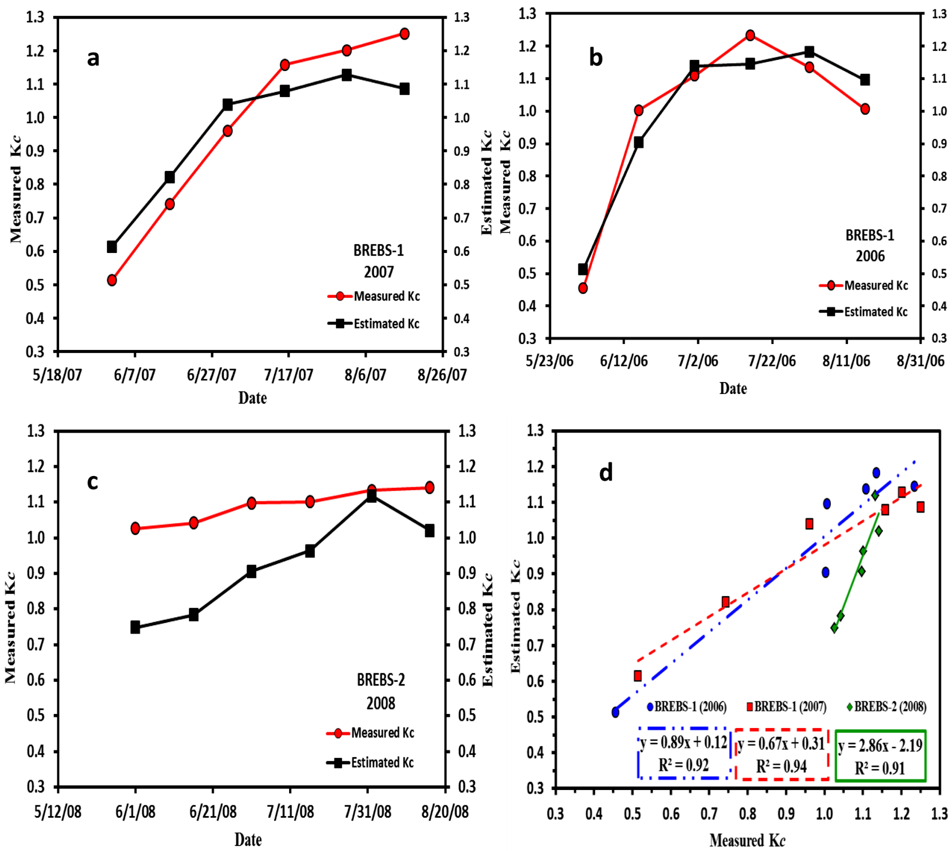

Figure 5. Growing season progression of NDVI and K*c* for the validation years in (a) 2007 and (b) 2006 at the NEBFLUX BREBS-1 site and in (c) 2008 at the NEBFLUX BREBS-2 site and (d) pooled data.

growing season ET*c* at the six locations were plotted on two graphs and presented in Figures 7a and 7b. The trend lines are shown on the figures as regression dashed lines. Figure 7a shows the increasing growing season ET*c* trends at four locations. Although the trends are increasing, the slopes at Loc-D (1.3), Loc-F (1.91), and Loc-C (1.42) were not significant ($p > 0.05$). However, the slope at Loc-B (2.28) was increasing significantly ($p < 0.05$). Figure 7b shows the growing season ET*c* with almost zero trends; the slopes at Loc-E and Loc-A were 0.49 and −0.52, respectively, both of which were insignificant. There is natural noise in the results due to the several severe droughts (1985, 1987–1989, 1999–2000, and 2002) that impacted the region in the last 30 years, possibly masking the significance of the trends in the short-term periods. Despite the noise in ET*c*, the results appear to indicate an increase in ET*c* fluxes during the study period. Since no increasing trends were evident in ET*o* (Figure 4), the probable explanation for the increase in ET*c* trends was attributed to the increase in irrigation practices and agronomic vegetation coverage. This increase in irrigation practices over the past three decades has sustained a steady increase in well-watered vegetation surface in the High Plains that potentially increased transpirative losses and atmospheric water vapor.

[21] In the High Plains, irrigation development has increased significantly over the past 5–6 decades. Figure 8 shows that irrigated acreage in the High Plains States increased from about 8×10^6 ha in 1980 to more than 13.4 $\times 10^6$ ha in 2000. This trend has continued into the 21st century as economical profitability and other incentives of maize, soybean, wheat, and other commodity crops have led farmers to convert natural vegetation surfaces (i.e., grasslands) into irrigated fields. *Irmak* [2010] reported that, based on the irrigation survey conducted by the USDA, Nebraska, total irrigated area has increased by 40% from about 1.6×10^6 ha in 1970 to over 3.6×10^6 ha in 2008. Thus, the increasing trend in ET*c* flux over the High Plains is not from increased atmospheric evaporative demand (ET*o*). Rather, the primary reason for the increase in ET*c* fluxes is due to increased irrigated area as rainfed croplands and natural grasslands are converted into irrigated fields. Thus, over the past 30 years, there has been an increase in well-watered vegetation surface with the potential of meeting the daily crop water requirements. To further evaluate this point, we plotted the percentage area of the High Plains, which had NDVI greater than 0.70 during the second half of July from 1981 to 2008 (Figure 9). NDVI saturates at high green biomass; therefore, the study considered values greater than 0.70 as densely vegetated surfaces, most likely with a full canopy cover. Figure 9 reveals an increase in spatial distribution of NDVI greater than 0.70 in the early 1980s; however, the increasing trend was impacted by the 1987–1989 droughts. From 1990, NDVI

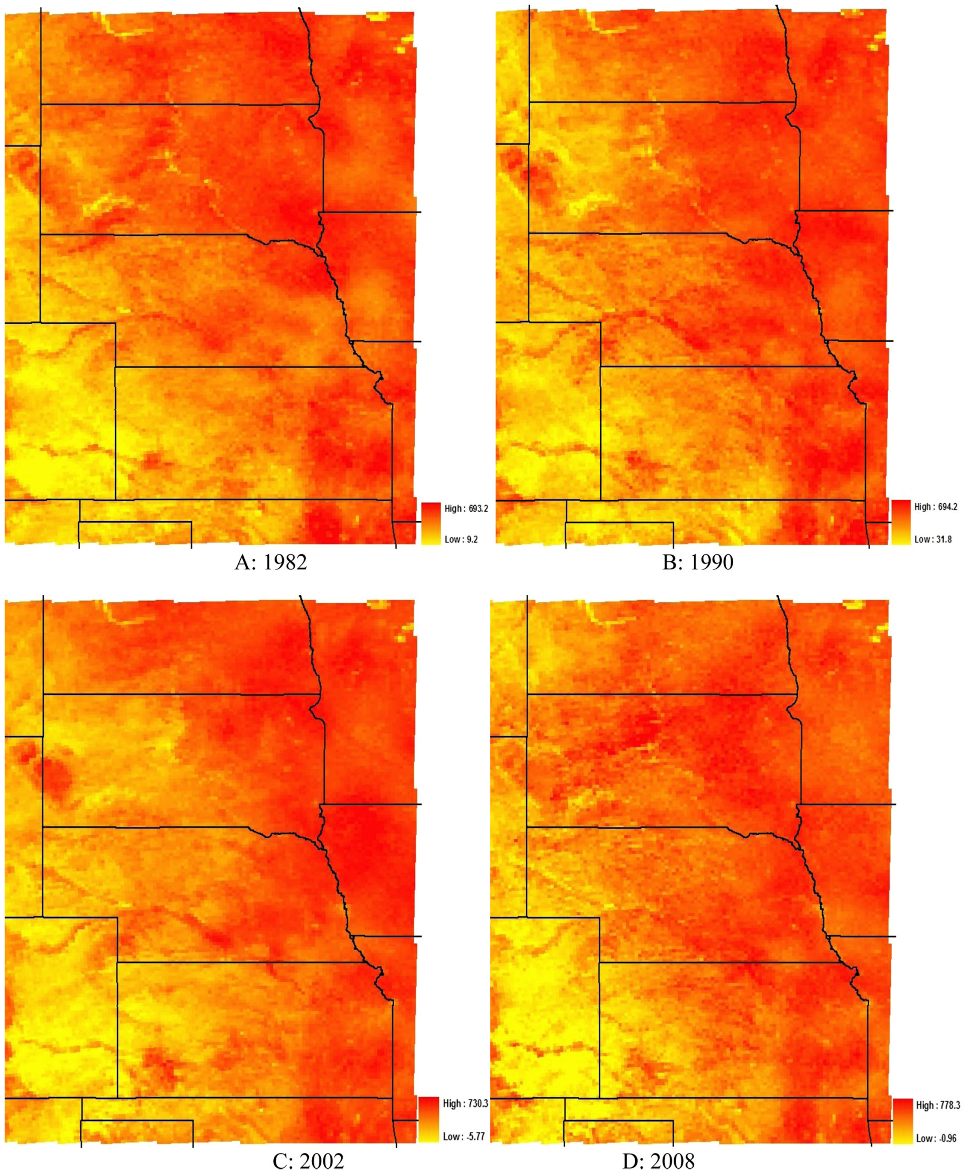

Figure 6. Spatial distribution of growing season ET*c* (mm) in the High Plains for 1982, 1990, 2002, and 2008.

increased until 1994, when it remained relatively stable until 2001. A comparison between the period of the early 1980s and the period from 1992 until 2008 indicates that there has been an increase in full canopy cover vegetation surfaces in the High Plains. The consistent increase in full canopy cover vegetation surfaces, even during dry and warm peak summer months, is attributed to increased irrigation practices.

[22] Several studies [*Kueppers et al.*, 2007; *Lobell et al.*, 2009; *Adegoke et al.*, 2003; *Boucher et al.*, 2004] have indicated that irrigation and vegetation coverage have direct influence on regional surface temperatures. *Segal et al.* [1988] reported a substantial persistence of surface temperature gradients over 10°C as observed from a satellite, due to landscape differences, including irrigated cropland adjacent to a natural short grass prairie in Colorado. An increase in ET*c* fluxes could indicate an increase in partitioning of surface energy into latent heat and decrease of available surface energy toward sensible heat. The decrease in sensible heat is expressed and measured as decrease in surface temperatures. *Mutiibwa* [2011] showed that the temperatures in the High Plains, especially in the central part, have been impacted by regional evaporative cooling. In Figure 9, we graphed the percentage area of the High Plains with NDVI values greater than 0.70 and the maximum temperature anomalies. The maximum temperature anomalies revealed a statistically significant strong negative autocorrelation of −0.424 with NDVI trend during the study period. The warmest temperatures were observed in 1988 during the peak of the 1987–1989 droughts. The temperature cooled in 1992 following the global cooling due to the Mt. Pinatubo eruption in the Philippines [*Hansen et al.*, 1992]. Since 1990, the temperatures recovered but never increased much until the droughts of 1999–2000 and 2002, which impacted the region substantially. *Lobell et al.* [2008] studied trends in maximum temperature and observed

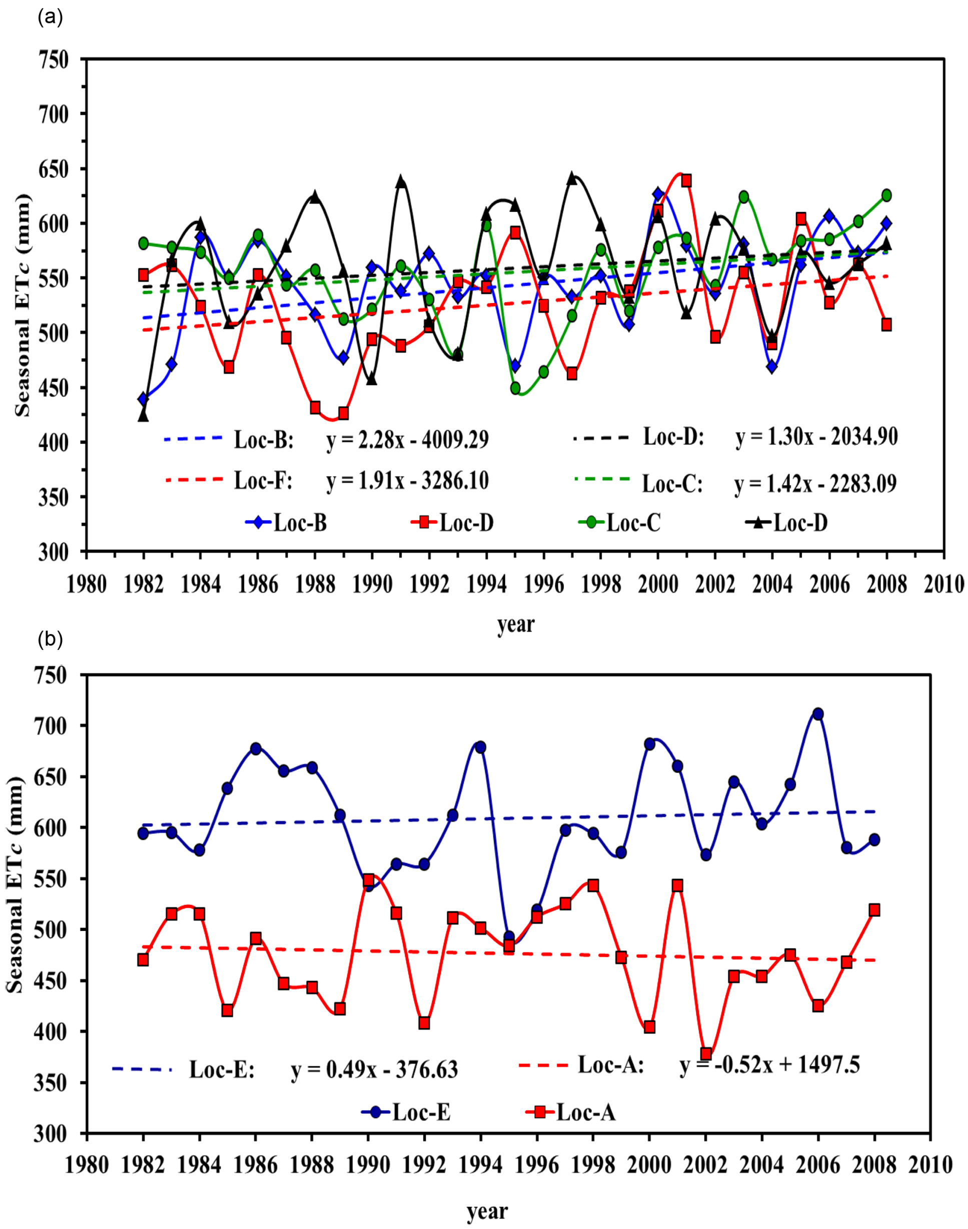

Figure 7. (a) Growing season ET*c* evolution during the study period at four sample locations with discernible increasing trends. The dashed regression lines represent the trend in ET*c* during the study period (1981–2008). (b) Growing season ET*c* evolution during the study period at two sample locations with no discernible trends in the High Plains. The black dotted lines show the possible trend line in ET*c* during the study period (1981–2008).

negative trends in the irrigated areas of Nebraska, which were attributed to increase in latent heat flux and corresponding reduction in sensible heat flux. *Oke* [1989] refers to such effect as local anthropogenic cooling from increasing irrigation and vegetation coverage. The strong negative relation between maximum temperature and NDVI is an indication of the regional evaporative cooling signal from irrigation that is also imbedded on the regional temperatures.

4. Conclusions

[23] This study proposed a global relationship between K*c* and NDVI and estimated spatial ET*o* and spatial growing season ET*c* for the High Plains region of the United States. The ET*c* flux at 8 km grid and biweekly temporal resolution were estimated using the two-step approach. The study examined the trends of ET*o* during the study period and found no evident increasing or decreasing trends. The spatial growing season ET*c*, however, shows an increasing pattern from the central to the eastern part of the High Plains region. The trends in growing season ET*c* appear to depict an overall increase in ET*c* fluxes over the High Plains. Because there was no increasing trend in ET*o*, the observed increase in ET*c* fluxes was attributed to increase in extensive irrigation practices and vegetation coverage during the study period, specifically during the summer

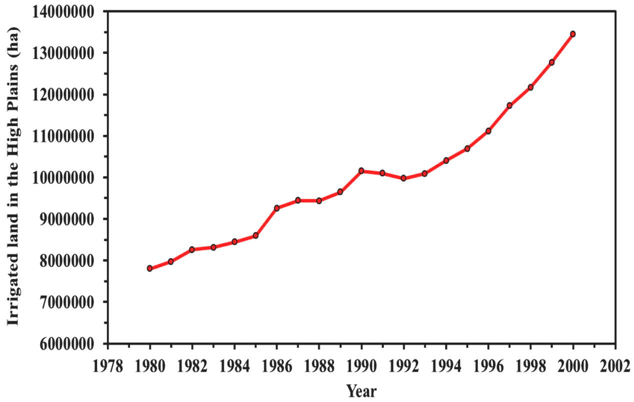

Figure 8. Trend showing substantial increase in total irrigated acreage in the U.S. High Plains states since 1980.

months. The Irrigated land area in the High Plains increased by 5.4×10^6 ha from 1980 to 2000, and the trend has continued to today. The increasing trend in ET*c* fluxes is a measure of increased partitioning of the surface available energy into latent heat and less energy partitioning into the sensible heat resulting in cooling of regional temperatures. The evolution of full canopy cover vegetation (NDVI > 0.70) in relation to the maximum temperature anomalies during the study period revealed a significant negative correlation between the two variables. These results appear to demonstrate that there is a regional evaporative cooling signal due to extensive irrigation practices, which is implicitly imbedded into the regional temperatures of the High Plains. The global relationship we proposed between K*c* and NDVI is a result of only 3 year measurements, but it was applied to the 27 year study period that has significantly different climate and surface characteristics than the K*c*-NDVI calibration years. Thus, the robustness of the relationship should be further researched in different climatic and surface conditions. Furthermore, developing crop (surface)-specific, rather than global, K*c*-NDVI relationship could enhance the accuracy in estimating K*c* values.

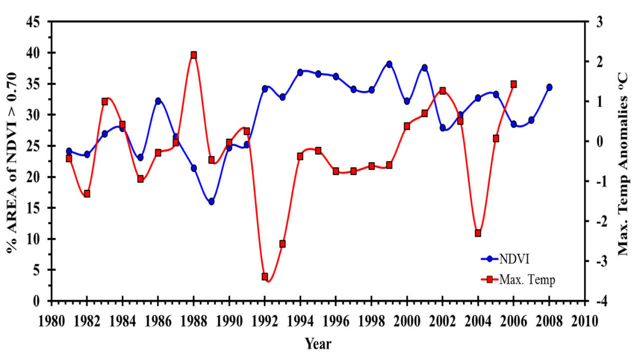

Figure 9. Evolution of percentage area of NDVI greater than 0.7 and the average maximum temperature anomalies for the months of June–August from 1981 to 2006 over the High Plains.

References

Adegoke, J. O., R. A. Pielke, J. Eastman, R. Mahmood, and K. G. Hubbard (2003), Impact of irrigation on midsummer surface fluxes and temperature under dry synoptic conditions: A regional atmospheric model study of the US High Plains, *Mon. Weather Rev.*, *131*, 556–564.

Boucher, O., G. Myhre, and A. Myhre (2004), Direct human influence of irrigation on atmospheric water vapour and climate, *Clim. Dyn.*, *22*, 597–603.

Doorenbos, J., and W. O. Pruitt (1979), *Crop Water Requirements. Irrigation and Drainage Paper No. 24 (Revised)*, Food and Agricultural Organization of the United Nations (FAO), Rome, Italy.

Folland, C. K., et al. (2001), Global temperature change and its uncertainties, *Geophys. Res. Lett.*, *28*, 2621–2624, doi:10.1029/2001GL012877.

Hansen, J., A. Lacis, R. Ruedy, and M. Sato (1992), Potential climate impact of Mount Pinatubo eruption, *Geophys. Res. Lett.*, *19*, 215–218.

Hargreaves, G. H., and Z. A. Samani (1982), Estimating potential evapotranspiration, *J. Irrig. Drain. Div. Am. Soc. Civ. Eng.*, *108*(3), 225–230.

Hargreaves, G. L., and Z. A. Samani (1985), Reference crop evapotranspiration from temperature, *Appl. Eng. Agric.*, *1*(2), 96–99.

Hunsaker, D. J., P. J. Pinter Jr., and B. A. Kimball (2005), Wheat basal crop coefficients determined by normalized difference vegetation index, *Irrig. Sci.*, *24*, 1–14.

Irmak, S. (2010), Nebraska water and energy flux measurement, modeling, and research network (NEBFLUX), *Trans. ASABE*, *53*, 1097–1115.

Irmak, S., I. Kabenge, K. Skaggs, and D. Mutiibwa (2012), Trend and magnitude of changes in climate variables and reference evapotranspiration over 116-year period in the Platte River Basin, central Nebraska-USA, *J. Hydrol.*, *420–421*, 228–244.

Kueppers, L. M., M. A. Snyder, and L. C. Sloan (2007), Irrigation cooling effect: Regional climate forcing by land-use change, *Geophys. Res. Lett.*, *34*, L03703, doi:10.1029/2006GL028679.

Lobell, D., G. Bala, A. Mirin, T. Phillips, and R. Maxwell (2009), Regional differences in the influence of irrigation on climate, *J. Climate.*, *22*, 2248–2255.

Lobell, D. B., C. J. Bonfils, L. M. Kueppers, and M. A. Snyder (2008), Irrigation cooling effect on temperature and heat index extremes, *Geophys. Res. Lett.*, *35*, L09705, doi:10.1029/2008GL034145.

Neale, C. M. U., W. C. Bausch, and D. F. Heerman (1989), Development of reflectance-based crop coefficients for corn, *Trans. ASAE*, *32*, 1891–1899.

Oke, T. R. (1989), The micrometeorology of urban forest, *Philos. Trans. R. Soc. B.*, *324*, 335–349.

Pan, Z., R. W. Arritt, E. S. Takel, W. J. Gutowski Jr., C. J. Anderson, and M. Segal (2004), Altered hydrologic feedback in a warming climate introduces a "warming hole," *Geophys. Res. Lett.*, *31*, L17109, doi:10.1029/2004GL020528.

Peterson, T. C., and R. C. Vose (1997), An overview of the global historical climatology network temperature data base, *Bull. Am. Meteorol. Soc.*, *78*(12), 2837–2849.

Pielke, R. A. G., Sr., G. Marland, R. A. Betts, T. N. Chase, J. L. Eastman, J. O. Niles, D. D. S. Niyogi, and S. W. Running (2002), The influence of land-use change and landscape dynamics on the climate system: Relevance to climate-change policy beyond the radiative effect of greenhouse gases, *Philos. Trans. R. Soc. A*, *360*, 1705–1719.

Pinzon, J., M. E. Brown, and C. J. Tucker (2004), Satellite time series correction of orbital drift artifacts using empirical mode decomposition, in *Hilbert-Huang Transform: Introduction and Applications*, edited by N. E. Huang and S. S. Shen, chap. 10, Part II, World Scientific, Singapore, pp. 167–186.

Rhodes, S. L., and S. E. Wheeler (1996), Rural electrification and irrigation in the U.S. High Plains, *J. Rural Stud.*, *12*, 311–317.

Riebsame, W. E., S. A. Changnon, and T. R. Karl (1991), *Drought and Natural Resources Management in the United States: Impacts and Implications of the 1987–89 Drought*, Westview, Boulder, Colo.

Rossum, S., and S. Lavin (2000), Where are the Great Plains? A cartographic analysis, *Prof. Geogr.*, *52*, 543–552.

Segal, M., R. Avissar, M. C. McCumber, and R. A. Pielke (1988), Evaluation of vegetation effects on the generation and modification of mesoscale circulations, *J. Atmos. Sci.*, *45*, 2268–2292.

Singh, R. K., and A. Irmak (2009), Estimation of crop coefficients using satellite remote sensing, *J. Irrig. Drain. Eng.*, *135*(5), 597–608.

Smith T. M., R. W. Reynolds, T. C. Peterson, and J. Lawrimore (2008), Improvements to NOAA's historical merged land-ocean surface temperature analysis (1880–2006). *J. Clim.*, *21*, 2283–2293.

Tucker, C. J., J. E. Pinzon, M. E. Brown, D. Slayback, E. W. Pak, R. Mahoney, E. Vermote, and E. S. Nazmi (2005), An extended AVHRR 8-km NDVI dataset compatible with MODIS and SPOT vegetation NDVI data, *Int. J. Remote Sens.*, *26*, 4485–4498.

Waltman, J. W., M. S. Goddard, S. E. Reichenbach, M. Svoboda, M. Hayes, and J. S. Peake (2003), Climate regimes and drought events in the northern great plains, presented at the CSE Conference and Workshop Paper, Applied Geography Conference, Univ. of Lincoln, Nebr.

Willmott, C. J. (1982), Some comments on the evaluation of model performance, *Bull. Am. Meteorol. Soc.*, *63*, 1309–1313.

Wright, J. L. (1982), New evapotranspiration crop coefficients, *J. Irrig. Drain. Div. Am. Soc. Civ. Eng.*, *108*, 57–74.

Xu, C. Y., and V. P. Singh (2001), Evaluation and generalization of temperature-based methods for calculating evaporation, *Hydrol. Processes*, *15*, 305–319.